THE JOURNAL OF BIOLOGICAL CHEMISTRY VOL. 285, NO. 41, pp. 31348–31361, October 8, 2010

Glycosylation of β2 Subunits Regulates $GABA_A$ Receptor Biogenesis and Channel Gating*[S]

Received for publication, June 3, 2010, and in revised form, July 7, 2010 Published, JBC Papers in Press, July 16, 2010, DOI 10.1074/jbc.M110.151449

Wen-yi Lo[‡§], Andre H. Lagrange[‡], Ciria C. Hernandez[‡], Rebecca Harrison[¶], Anne Dell[¶], Stuart M. Haslam[¶], Jonathan H. Sheehan[‖], and Robert L. Macdonald[‡ ‡‡§§1]**

*From the Departments of [‡]Neurology, [‖]Biochemistry, [‡‡]Molecular Physiology and Biophysics, and [§§]Pharmacology, [§]Program in Neuroscience, and **Center for Structural Biology, Vanderbilt University, Nashville, Tennessee 37232 and the [¶]Division of Molecular Biosciences, Imperial College London, London SW7 2AZ, United Kingdom*

γ-Aminobutyric acid type A ($GABA_A$) receptors are heteropentameric glycoproteins. Based on consensus sequences, the $GABA_A$ receptor β2 subunit contains three potential *N*-linked glycosylation sites, Asn-32, Asn-104, and Asn-173. Homology modeling indicates that Asn-32 and Asn-104 are located before the α1 helix and in loop L3, respectively, near the top of the subunit-subunit interface on the minus side, and that Asn-173 is located in the Cys-loop near the bottom of the subunit N-terminal domain. Using site-directed mutagenesis, we demonstrated that all predicted β2 subunit glycosylation sites were glycosylated in transfected HEK293T cells. Glycosylation of each site, however, produced specific changes in α1β2 receptor surface expression and function. Although glycosylation of Asn-173 in the Cys-loop was important for stability of β2 subunits when expressed alone, results obtained with flow cytometry, brefeldin A treatment, and endo-β-*N*-acetylglucosaminidase H digestion suggested that glycosylation of Asn-104 was required for efficient α1β2 receptor assembly and/or stability in the endoplasmic reticulum. Patch clamp recording revealed that mutation of each site to prevent glycosylation decreased peak α1β2 receptor current amplitudes and altered the gating properties of α1β2 receptor channels by reducing mean open time due to a reduction in the proportion of long open states. In addition to functional heterogeneity, endo-β-*N*-acetylglucosaminidase H digestion and glycomic profiling revealed that surface β2 subunit *N*-glycans at Asn-173 were high mannose forms that were different from those of Asn-32 and N104. Using a homology model of the pentameric extracellular domain of α1β2 channel, we propose mechanisms for regulation of $GABA_A$ receptors by glycosylation.

N-Linked glycosylation plays a pivotal role in biogenesis and functions of secreted and membrane proteins, including ligand-gated ion channels. Mutations of enzymes involved in the *N*-linked glycosylation pathway have been associated with congenital disorders of glycosylation, many of which cause psychomotor retardation and seizures (1). The Cys-loop receptor superfamily of ligand-gated ion channels, which contains γ-aminobutyric acid type A ($GABA_A$),[2] nicotinic acetylcholine (nACh), glycine, and 5-hydroxytryptamine type 3 ($5\text{-}HT_3$) receptors, mediates fast synaptic transmission in the nervous system and is involved in nearly every aspect of brain activity. It has been shown that blocking *N*-linked glycosylation of Cys-loop receptors using tunicamycin substantially decreased receptors surface expression (2–4).

$GABA_A$ receptor β1–3 subunits are essential components of virtually all $GABA_A$ receptors expressed in brain (5, 6). Based on the glycosylation sequons, Asn-Xaa-Ser/Thr, where Xaa is any amino acid except proline (7), each subunit contains three potential glycosylation sites in equivalent positions (Asn-32, Asn-104, and Asn-173 in the β2 subunit). Furthermore, multiple sequence alignment using Multalin software (8) and homology modeling suggested that about three quarters of all human Cys-loop receptor subunits contain potential glycosylation sites in the region containing the Asn-32 site, and about one-half of the subunits contain potential glycosylation sites in the region containing the Asn-104 or Asn-173 sites (Table 1). The clustering of the glycosylation sites in Cys-loop receptor subunits further suggests that *N*-linked glycosylation might regulate Cys-loop receptor biogenesis and functions similarly in a spatially related manner. In support of this prediction, an intact Asn-32 equivalent site of the $GABA_A$ receptor α1 subunit or the nACh receptor α7 subunit (9, 10), an intact Asn-104 equivalent site of the nACh receptor α7 subunit or the mouse $5\text{-}HT_3$ A subunit (4, 10), and an intact Asn-173 equivalent site of the mouse nACh receptor α1 subunit or the $5\text{-}HT_3$ A subunit are required for functional receptor surface expression (4, 11).

In this study we determined the importance of glycosylation of β2 subunits for surface targeting and function of α1β2 receptors in transfected human embryonic kidney (HEK293T) cells. We demonstrated that glycosylation efficiency of Asn-32 was lower than Asn-104 or Asn-173. Although glycosylation of Asn-173 was important for stability of singly expressed sub-

* This work was supported, in whole or in part, by National Institutes of Health Grants R01 NS51590 (to R. L. M.) and K08 NS045122 (to A. H. L.). This work was also supported by the Biotechnology and Biological Sciences Research Council (to A. D. and S. M. H.) and a Departmental Training Account Studentship from the Biotechnology and Biological Sciences Research Council (to R. H.).

[S] The on-line version of this article (available at http://www.jbc.org) contains supplemental Figs. 1–3.

[1] To whom correspondence should be addressed: Vanderbilt University Medical Center, 6140 Medical Research Bldg. III, 465, 21st Ave., Nashville, TN 37232-8552. Tel.: 615-936-2287; Fax: 615-322-5517; E-mail: robert.macdonald@vanderbilt.edu.

[2] The abbreviations used are: $GABA_A$, γ-aminobutyric acid type A; endo H, endo-β-*N*-acetylglucosaminidase H; nACh, nicotinic acetylcholine; ER, endoplasmic reticulum; IDV, integrated density volume; PE, R-phycoerythrin; PNGase F, peptide *N*-glycosidase F; $5\text{-}HT_3$, 5-hydroxytryptamine type 3.

TABLE 1

Subunits that contain potential *N*-linked glycosylation sites around the α1 helix, in the L3, or in the L7 element

Numbers in parentheses and the last row indicate subunits within a given human Cys-loop receptor family and the whole superfamily, respectively, which have potential glycosylation sites around the α1 helix, in the L3, or in the L7 element.

	Around α1 helix (Asn-32)	In L3 (Asn-104)	In L7 (Asn-173)
$GABA_A$ receptors	α1–6, β1–3, γ1–2, π (12/16)	β1–3, γ1–3, δ, ϵ, θ, π (10/16)	β1–3 (3/16)
$GABA_C$ receptors	None (0/3)	ρ1–3 (3/3)	ρ3 (1/3)
Glycine receptors	α1–4, β (5/5)	None (0/5)	None (0/5)
Nicotinic acetylcholine[a] receptors	α2, α4, α6–7, α9–10, β2–4, γ (10/16)	α2–4, α7, β4, δ, ϵ (7/16)	α1, α3–6, α9, β1–4, γ δ, ϵ (13/16)
$5\text{-}HT_3$ receptors	$5\text{-}HT_{3A-F}$ (5/5)	$5\text{-}HT_{3A-B}$ (2/5)	$5\text{-}HT_{3A-F}$ (5/5)
Total	32/45	22/45	22/45

[a] α1, α5, and β1 are the only three subunits in the human Cys-loop superfamily that contain no glycosylation sites either around α1 helix or L3 element.

units, Asn-104 was the principal glycosylation site responsible for pentameric α1β2 receptor assembly and/or stability in the endoplasmic reticulum (ER). Additionally, mutation of any of the three glycosylation sites decreased α1β2 receptor peak current amplitudes and reduced the proportion of long-lived single channel openings. Using a homology model of the pentameric extracellular N-terminal domain of α1β2 receptors, we further proposed mechanisms of regulation of receptor biogenesis and channel gating by β2 subunit glycosylation.

EXPERIMENTAL PROCEDURES

DNA Constructs—A complementary DNA (cDNA) encoding human $GABA_A$ receptor α1 or β2 subunit polypeptide was inserted into the pcDNA3.1(+) vector. The FLAG epitope, DYKDDDDK, was introduced between the eighth and ninth amino acids of the α1 subunit polypeptide or between the fourth and fifth amino acids of the β2 subunit polypeptide (numbered excluding the signal peptide). The epitope insertion at these positions has been demonstrated to cause no significant changes in electrophysiological properties or surface levels of α1β2 receptors (2, 12). The QuikChange site-directed mutagenesis kit (Stratagene) was used to make subunits with segmental deletions or point mutations. The $\alpha1(\text{loop}\Delta)^{FLAG}$ subunit was constructed by deleting the first half of the major cytoplasmic loop between the TM3 and TM4 domains, Asn–335—Leu–386, of the FLAG-tagged α1 subunit. The potential β2 subunit glycosylation sites, Asn-32, Asn-104, or Asn-173 (numbered including the signal peptide), were mutated to other amino acids.

Cell Culture and Transfection—HEK293T cells were incubated at 37 °C in 5% CO_2, 95% air and grown in Dulbecco's modified Eagle's medium (Invitrogen) supplemented with 10% fetal bovine serum (Invitrogen) plus 100 IU/ml each of penicillin and streptomycin (Invitrogen). Altogether, 1 μg each of α1 and β2 subunit plasmids were mixed with 6 μl of FuGENE 6 transfection reagent (Roche Applied Science) and incubated with 4×10^5 cells in a 60-mm diameter culture dish. For whole cell recording, plasmids were introduced into cells using the modified calcium phosphate precipitation method (13). For mock or single subunit expression, empty vector was added so as the total mass of DNA transfected was 2 μg. When using culture dishes of different sizes, the DNA-FuGENE 6 mixture volumes were scaled up or down proportionally to the culture dish surface areas. To select for positively transfected cells for electrophysiological experiments, pHook-1, a plasmid encoding a single-chain antibody (Invitrogen), or GFP plasmid in the amount of ⅙ or 1% of the total mass of subunit plasmids was cotransfected, respectively. Cells expressing the single-chain antibody were selected using immunomagnetic beads 1 day after transfection and were recorded 1 day after selection (14). Unless otherwise specified, cells were used for experiments 48 h after transfection.

Western Blots—Transfected HEK293T cells were broken by freeze-and-thaw cycles. The cytoplasmic fraction was then separated by centrifugation. The pellet containing the membrane fraction was extracted using radioimmune precipitation assay buffers, which contained 50 mM Tris-HCl (pH 7.4), 150 mM NaCl, 1 mM EDTA, 1–2% Nonidet P-40, 0.25–0.5% sodium deoxycholate, and protease inhibitor mixture (Sigma). Insoluble components were removed by centrifugation at 16,000 × *g* for 30 min. The supernatants were subjected to further experiments or directly to SDS-PAGE. Proteins in gels were transferred to polyvinylidene fluoride membranes (Millipore).

A monoclonal anti-$GABA_A$ receptor α1 subunit antibody (final concentration 5 μg/ml; clone: BD24, Millipore) was used to detect α1 subunits, and a monoclonal anti-$GABA_A$ receptor β2/3 antibody (4 μg/ml; clone: 62–3G1, Millipore) or polyclonal rabbit anti-$GABA_A$ receptor β2 antibody (0.2 μg/ml; Millipore) was used to detect control (wild-type subunits in the control condition) or mutant human β2 subunits. The monoclonal anti-$GABA_A$ receptor β2/3 antibody was used to evaluate molecular masses but was not used to compare surface or total levels of mutant β2 subunits because mutations at glycosylation sites affected anti-β2 subunit antibody affinity (supplemental Fig. 1). An anti-sodium potassium ATPase (Na^+/K^+-ATPase) antibody (0.2 μg/ml; clone ab7671, Abcam) was used as a loading control. After incubation with primary antibodies, secondary goat anti-mouse or anti-rabbit IgG heavy and light chain antibodies conjugated with horseradish peroxidase were used at a 1:10,000× dilution (Jackson ImmunoResearch Laboratories) for visualization of specific bands in enhanced chemiluminescence detection system (Amersham Biosciences).

The signals were collected in a digital ChemImager (Alpha Innotech). The integrated density volumes (IDV; pixel intensity × mm^2) were then calculated using the FluorChem 5500 software. Adjusted IDVs (normalized to loading control Na^+/K^+-ATPase IDVs) of mutant and partnering subunits were expressed as the % of adjusted IDVs of corresponding control subunits. Data were expressed as the mean ± S.D.

Surface Expression Measurement Using Flow Cytometry—Measurement of surface expression of $GABA_A$ receptor subunits using flow cytometry has been described previously (12). Briefly, transfected HEK293T cells were removed from the

dishes by trypsinization and then resuspended in FACS buffer (phosphate-buffered saline (PBS) supplemented with 2% FBS and 0.05% sodium azide). After washes with FACS buffer, cells were incubated with anti-FLAG IgG directly conjugated with R-phycoerythrin (PE, 1:50 dilution, Martek) for 1 h at 0 °C. Cells were then washed with FACS buffer and fixed with 2% paraformaldehyde. The surface fluorescence intensity of each cell was measured using a FACSCalibur (BD Biosciences).

The acquired data were analyzed using FlowJo 7.1 (Treestar, Inc.). Mean fluorescence of the viable population, which excluded 7-amino-actinomycin D (Invitrogen), of a given experimental condition was obtained. To account for cell autofluorescence and nonspecific staining, mean fluorescence of viable cells with mock transfection (transfected with empty vector, pcDNA3.1(+)) was subtracted from that obtained in each experimental condition. For comparison among various experimental conditions, the mock-subtracted mean fluorescence values for each experimental condition were expressed as a percentage of those with control subunit coexpression. Data were expressed as the mean ± S.D.

Brefeldin A Treatment—Brefeldin A has been used to block ER forward trafficking and, thus, subsequent surface expression of fully assembled $GABA_A$ receptors (12). HEK293T cells were treated with 0.5 μg/ml brefeldin A (Sigma) 6 h after transfection and then harvested 24 h after transfection. Total levels of expressed $GABA_A$ receptor subunits were then measured using Western blots.

Biotinylation of Cell Surface Proteins—HEK293T cell surface proteins were biotinylated with membrane-impermeable reagent sulfo-NHS-SS-biotin (1 mg/ml, Thermo Scientific) in PBS containing 0.1 mM $CaCl_2$ and 1 mM $MgCl_2$ (PBS+CM) at 4 °C for 1 h. After incubation, the biotin was quenched with 0.1 M glycine in PBS+CM. After washes with PBS+CM, cells were lysed in radioimmune precipitation assay buffer supplemented with protease inhibitors (Sigma). After centrifugation to pellet cellular debris, the biotin-labeled plasma membrane proteins were pulled down by streptavidin beads (Thermo Scientific) at 4 °C overnight.

Glycosidase Digestions—HEK293T cell proteins in the membrane fraction or surface-biotinylated proteins were subjected to endo-β-*N*-acetylglucosaminidase H (endo H) or peptide *N*-glycosidase F (PNGase F) digestion (New England Biolabs) at 37 °C for 3 h.

Glycomic Profiling of N-Glycans of Surface β2 Subunits with Coexpression of α1(loopΔ)^{FLAG} Subunits—To facilitate distinguishing between α1 and β2 subunits during sample purification, α1(loopΔ)^{FLAG} subunits were used to express binary receptors. Surface proteins of HEK cells with α1(loopΔ)^{FLAG}β2, α1(loopΔ)^{FLAG}β2(N32Q), or α1(loopΔ)^{FLAG}β2(N173Q) subunit coexpression were biotinylated and subjected to two-step purification. First, FLAG-tagged α1(loopΔ) subunits and associated control or mutant β2 subunits were immunoprecipitated using anti-FLAG M2 beads (Sigma) at 4 °C overnight and were eluted with 100 μg/ml FLAG peptide (Sigma). To enrich the surface receptors, the eluted fraction was then subjected to pulldown by streptavidin beads at 4 °C overnight. After six washes, control or mutant β2 subunits in surface $GABA_A$ receptor complexes were separated from α1(loopΔ)^{FLAG} subunits by SDS-PAGE and subjected to glycomic analysis.

Each Coomassie Blue-stained gel band was destained using 100% acetonitrile and incubated with 10 mM dithiothreitol for 30 min at 56 °C. Iodoacetic acid was then added to a final concentration of 55 mM, in which the gel band was incubated for 30 min at room temperature. Each reduced and carboxymethylated protein was digested with 0.5 μg of sequencing grade-modified trypsin (EC 3.4.21.4; Sigma) at 37 °C for 14 h. Tryptic-digested peptides and glycopeptides were extracted from the gel piece by incubating with 0.1% trifluoroacetic acid and 100% acetonitrile. The supernatant was lyophilized before being dissolved in 200 μl of ammonium bicarbonate (50 mM (pH 8.4)) and incubated with 5 units of PNGase F (EC 3.5.1.52; Roche Applied Science) at 37 °C for 20 h. The reaction was terminated by lyophilization. *N*-glycans were separated from the peptides by C_{18} Sep-Pak (Waters) purification, permethylated (15), and analyzed by MALDI-TOF MS as previously described (16).

Recording and Analysis of Macroscopic GABA Evoked Currents—As described before (17), voltage-clamp whole cell recordings were performed on transfected HEK293T cells bathed in an external solution consisting of 142 mM NaCl, 8 mM KCl, 6 mM $MgCl_2$, 1 mM $CaCl_2$, 10 mM glucose, and 10 mM HEPES (pH 7.4, 320–330 mosM, *i.e.* milliosmolar or milliosmole per liter). The glass electrodes were pulled from thin-walled borosilicate capillary glass (Fisher) on a P-2000 Quartz Micropipette Puller (Sutter Instruments), fire-polished to a resistance of 1–2 megaohms on an MF-830 Micro Forge (Narishige), and filled with an internal solution consisting of 153 mM KCl, 1 mM $MgCl_2$, 5 mM EGTA, 10 mM HEPES, and 2 mM MgATP (pH 7.3, 310 mosM, *i.e.* milliosmolar or milliosmole per liter). The Cl^- equilibrium potential across the cell membrane was close to zero with the combination of external and internal solutions. Cells were voltage-clamped at −20 mV using an Axopatch 200A amplifier (Axon Instrument). GABA was applied to the lifted cells using a rapid perfusion system (open tip exchange times <700 μs) consisting of multibarrel square glass connected to a Perfusion Fast-Step (Warner Instruments) that was commanded by Clampex 9.0 software (Axon Instrument).

Inward GABA-evoked macroscopic currents were low-pass filtered at 2 kHz and digitized at 5–10 kHz using Digidata 1322A. Their peak amplitudes were analyzed using Clampfit 9.0 (Axon Instruments). For GABA-evoked currents with peak amplitudes greater than 50 pA, deactivation time courses were fitted using the Levenberg-Marquardt least squared error method with up to six exponential components in the form $\sum A_i \exp(-t/\tau_i) + C$, where A_i and τ_i are the relative amplitude and the time constant of the *i*th component, respectively, t is the time, and C is the residual current at the end of fitting. Deactivation time courses were then evaluated by weighted time constant calculated with the following: $(\sum A_i \tau_i)/(\sum A_i)$. Data were expressed as the mean ± S.E.

Single-channel Recording and Data Analysis—Single-channel currents were recorded using the patch clamp technique in the cell-attached configuration (18). Cell-attached single-channel currents were recorded from HEK293T cells bathed in the external solution containing 140 mM NaCl, 5 mM KCl, 1 mM $MgCl_2$, 2 mM $CaCl_2$, 10 mM glucose, and 10 mM HEPES (pH

7.4). Glass electrodes were pulled from thick-walled borosilicate capillary glass (World Precision Instruments, Inc.) on a P-2000 Quartz Micropipette Puller (Sutter Instruments) and fire-polished to a resistance of 10–20 megaohms on an MF-830 Micro Forge (Narishige) before use. During recording, 1 mM GABA was present in the electrode solution containing 120 mM NaCl, 5 mM KCl, 10 mM $MgCl_2$, 0.1 mM $CaCl_2$, 10 mM glucose, and 10 mM HEPES (pH 7.4) (19). The electrode potential was held at +80 mV.

Single channel currents were amplified and low-pass-filtered at 2 kHz using an Axopatch 200B amplifier, digitized at 20 kHz using Digidata 1322A, and saved using pCLAMP 9 software (Axon Instruments). Data were analyzed using TAC (Bruxton) software. Open and closed events were analyzed using the 50% threshold detection method. All events were carefully checked visually before being accepted. Only patches showing no overlaps of simultaneous openings were accepted. Open and closed time histograms as well as amplitude histograms were generated using TACFit (Bruxton). Single-channel amplitudes (i) were calculated by fitting all-point histograms with single- or multi-Gaussian curves. The difference between the fitted "closed" and "open" peaks was taken as i. Duration histograms were fitted with exponential components in the form: $\sum(A_i/\tau_i)\exp(-t/\tau_i)$, where A_i and τ_i are the relative area and the time constant of the ith component, respectively, and t is the time. The mean open time was then calculated as follows: $\sum A_i\tau_i$ (20, 21). The number of components required to fit the duration histograms was increased until an additional component did not significantly improve the fit (20). All experiments were conducted at room temperature. Data were expressed as the mean ± S.E.

Homology Modeling—The polypeptide sequences of the human $GABA_A$ receptor α1 and β2 subunit N-terminal domains without the signal peptides were aligned with primary sequences extracted from the atomic structures of the N-terminal domain of the α1 subunit of mouse nicotinic acetylcholine receptors (RCSB PDB ID 2QC1) (11) and of the acetylcholine-binding protein (RCSB PDB ID 1I9B) (22) using MultAlin (8). Based on the multiple sequence alignment result (supplemental Fig. 2*A*), the primary sequence of the $GABA_A$ receptor α1 or β2 subunit N-terminal domain starting from its first glycosylation site, Asn-38—Ile-250, for the α1 subunit or Asn-32—Ile-242 for the β2 subunit was threaded into the atomic structure of the mouse nicotinic acetylcholine receptor α1 subunit N-terminal domain using the Swiss-PdbViewer (23). Each of the obtained homology models was then subjected to SWISS-MODEL (project mode) for loop-building, side-chain rotamer selection, and energy minimization (24).

Using the pentameric acetylcholine-binding protein structure as a scaffold, the homology models of $GABA_A$ receptor α1 and β2 subunit N-terminal domains were assembled in the order of α1-β2-β2-α1-β2 viewed counterclockwise from the synaptic cleft using the Swiss-Pdb Viewer. To remove the clashes between subunits, the assembled pentameric complex of the extracellular domain of the α1β2 $GABA_A$ receptor was energy-minimized using the ff99SB forcefield in AMBER 10 (25). The atomic structure of the *N*-glycan of the 2QC1 template attached to a site equivalent to $GABA_A$ receptor β2 subunit Asn-173 site was also linked to each Asn-173 site of the three β2 subunits in the energy-minimized structure. The whole structure then was further energy minimized using ff99SB and GLYCAM_06 forcefields (26, 27).

FIGURE 1. **The extracellular N-terminal domain sequences of mature human $GABA_A$ receptor β1–3 subunits share 85% sequence identity and contain three potential glycosylation sites.** Immature human $GABA_A$ receptor β1–3 subunit amino acid sequences were aligned using ClustalW2. The symbols *, :, and . indicate that amino acids in the column are identical, conserved, or semi-conserved, respectively. The *first* and *second arrowheads* indicate the predicted beginnings of the mature polypeptides with cleavage of signal peptides and of transmembrane domain one, respectively. Glycosylation sequons Asn-Xaa-Ser/Thr, where Xaa can be any amino acid except proline, are in *bold*. The cysteine pairs forming the signature Cys-loop disulfide bonds are highlighted in *gray*. The *boxed region* indicates epitopes in β2/3 subunits recognized by monoclonal 62–3G1 and BD17 antibodies. Of note, extracellular N-terminal domains of $GABA_A$ receptor β subunit orthologs (human, rat, and mouse) are highly conserved, and only amino acids in *reversed white color* are different from rat or mouse.

Statistic Analysis—One-way analysis of variance with Tukey's post-test was used to determine whether there were significant differences among different transfection conditions.

RESULTS

The Three β2 Subunit Glycosylation Sites Were Glycosylated—Inspection of the β2 subunit amino acid sequence revealed three potential glycosylation sites, Asn-32, Asn-104, and Asn-173 (Fig. 1). Because the consensus sequon is required, but not sufficient, for *N*-linked glycosylation (7), we first needed to determine whether or not each of the predicted glycosylation sites was actually glycosylated. To address the question, we made single Asn to Gln mutations (single-Q mutations) in β2 subunits at each potential glycosylation site to make mutant β2(N32Q), β2(N104Q), and β2(N173Q) subunits that were missing one of the potential glycosylation sites and then transfected HEK293T cells with either native β2 or mutant single-Q β2 subunits alone. Molecular mass analyses using a combination of SDS-PAGE and Western blotting revealed that each of the three sites was glycosylated as β2(N32Q), β2(N104Q), and β2(N173Q) subunits migrated mainly with molecular masses of 51, 51, and 52 kDa, respectively, that were lower than 54 kDa, the molecular mass of the major population of native β2 subunits (Fig. 2*A*, *lanes 2–5*).

To understand better how the addition of an *N*-glycan at each β2 subunit glycosylation site contributed to subunit

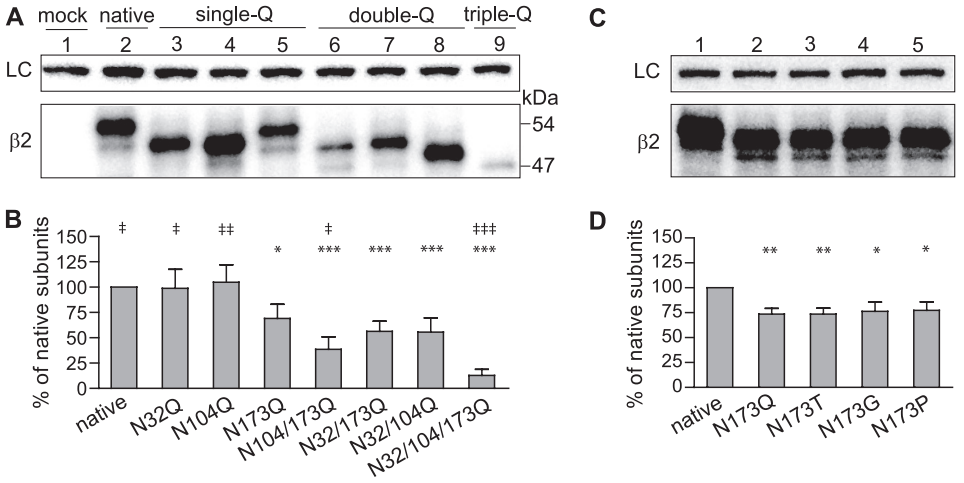

FIGURE 2. **In HEK293T cells all three predicted glycosylation sites were glycosylated, and glycosylation of Asn-173 was important for stability of β2 subunits expressed alone.** *A*, proteins in the membrane fraction of HEK293T cells transfected with empty vector (*mock*, *lane 1*) or plasmids encoding native β2 subunits (*native*, *lane 2*), mutant single-Q β2 subunits containing one mutated glycosylation site (N32Q, N104Q, or N173Q in *lane 3*, *4*, or *5*, respectively), mutant double-Q β2 subunits retaining only one glycosylation site (N104Q/N173Q, N32Q/N173Q, or N32Q/N104Q in *lane 6*, *7*, or *8*, respectively), or mutant triple-Q β2 subunits containing no glycosylation sites (N32Q/N104Q/N173Q, *lane 9*) were resolved by SDS-PAGE. The effects of altered glycosylation on molecular masses, and expression levels of mutant β2 subunits were evaluated using Western blots. The *upper panel* presents anti-Na^+/K^+-ATPase staining as a loading control (*LC*). The *lower panel* presents staining using anti-β2 subunit cytoplasmic loop antibodies. *B*, total-protein levels of mutant β2 subunits expressed alone with different combinations of glycosylation site mutations were quantified. The sums of all band densities of each lane, after being corrected for loading variation, were expressed as the % of the intensity of the native β2 subunits (*lane 2*). *C*, proteins in the membrane fraction of HEK293T cells transfected with native β2 subunits (*lane 1*) or mutant β2 subunits with the Asn-173 site mutated to glutamine (*Q*), threonine (*T*), glycine (*G*), or proline (*P*) (*lane 2*, *3*, *4*, or *5*, respectively) were resolved by SDS-PAGE. Proteins of interest were detected by Western blots. The *upper panel* presents anti-Na^+/K^+-ATPase staining as a loading control (*LC*). The *lower panel* presents anti-β2 subunit staining. *D*, total protein levels of mutant β2 subunits expressed alone were quantified. The sums of all band densities of each lane, after being corrected for loading variation, were expressed as the % of the intensity of the native β2 subunits (*lane 1*). Data are presented as the mean ± S.D. *, **, and *** indicate $p < 0.05$, $p < 0.01$, and $p < 0.001$, respectively, relative to the total level of the native β2 subunit. ‡, ‡‡, and ‡‡‡ indicate $p < 0.05$, $p < 0.01$, and $p < 0.001$, respectively, relative to the total level of the mutant single-Q β2(N173Q) subunit.

molecular mass, double Asn to Gln mutations (double-Q mutations) were also introduced into β2 subunits to make mutant β2(N104Q/N173Q), β2(N32Q/N173Q), and β2(N32Q/N104Q) subunits that had only one intact glycosylation site. Furthermore, a triple Asn to Gln mutation (triple-Q mutation) was introduced into the β2 subunit to make a mutant β2(N32Q/N104Q/N173Q) subunit with no glycosylation sites. Removal of all *N*-glycans from β2 subunits with the triple-Q mutation produced a single band with a molecular mass of 47 kDa (Fig. 2*A*; *lane 9*). The major bands of the three double-Q mutations, which retained only the Asn-32, Asn-104, or Asn-173 site, migrated with higher molecular masses of 50, 50, or 48 kDa, respectively. Taken together, the mobility shifts suggested that *N*-glycans at Asn-173 had a lower mass than those at Asn-32 or Asn-104 (Fig. 2*A*, *lanes 6–8*). The mass of the β2(N173Q) subunit was 2 kDa smaller than the native β2 subunits, but that of the β2(N32Q/N104Q) subunit, which retained Asn-173, was only 1 kDa greater than the unglycosylated triple-Q mutant subunits. This discrepancy in changes of molecular mass might be due to round-up errors. Additionally, we could not exclude the possibility that *N*-glycans attached to each site have similar molecular masses and deglycosylation of Asn-173 caused other effects that led to lower mobility shifts. The underlying mechanism responsible for the differences of mobility shifts after the glycosylation site mutations will require future investigation.

Glycosylation efficiency is regulated in part by the sequon sequences, particularly the hydroxyl amino acids, with the sequon Asn-Xaa-Thr being a stronger acceptor of *N*-glycans than Asn-Xaa-Ser (28–30). For β2 subunits, the first sequon, Asn-32–Met-Ser, is the only one with Ser as the hydroxyl amino acid (Fig. 1), suggesting that glycosylation of Asn-32 may be less efficient than of Asn-104 or Asn-173. Supporting this, 26% of double-Q β2(N104Q/N173Q) subunits, which contained only Asn-32 sites, migrated at a molecular mass equal to that of unglycosylated triple-Q β2 subunits ($n = 4$) (Fig. 2*A*, *lane 6*). Consistently, all other β2 subunits with an intact first glycosylation site also migrated at two molecular masses, *i.e.* native β2 and mutant β2(N104Q), β2(N173Q), and β2(N104Q/N173Q) subunits (Fig. 2*A*; *lanes 2* and *4–6*). Collectively, molecular mass analyses of mutant subunits expressed alone revealed that *N*-linked glycosylation of β2 subunits was structurally heterogeneous. The Asn-32 site had a lower glycosylation efficiency than the other two sites, and *N*-glycans attached to the Asn-173 site had lower molecular masses.

Glycosylation of the Third Glycosylation Site, Asn-173, Was Important for Stability of Singly Expressed Subunits—When expressed in the absence of partnering subunits, α1 and β2 subunits were retained in the ER and subsequently degraded by ER-associated degradation due to failure to assemble into homopentamers (12, 31). Furthermore, mutations of these subunits that affect biogenic steps earlier than heteropentameric assembly enhanced ER-associated degradation, resulting in a total mutant subunit level that was lower than that of singly expressed native subunits (32, 33). To determine whether or not blocking glycosylation at a specific β2 subunit glycosylation site destabilizes subunits and enhances subunit degradation in the absence of partnering subunits, total levels of singly expressed mutant β2 subunits were compared with those of native β2 subunits. Mutation of the first or second glycosylation site, Asn-32 or Asn-104, altered binding of the monoclonal 62–3G1 anti-β2/3 antibody (supplemental Fig. 1), and thus, we used rabbit polyclonal antibodies that recognized the major TM3-TM4 cytoplasmic loop of β2 subunits to determine expression levels.

Selectively abolishing glycosylation of the third glycosylation site with the N173Q mutation resulted in significantly lower total subunit levels (69%) compared with those of native subunits ($n = 5$; Fig. 2, *A* and *B*, *lanes 2–5*), suggesting that glyco-

sylation of the Asn-173 site was important for subunit stability. Subunit cDNAs were cloned into the same vector, and thus, the transcriptional and translational efficiency of mRNAs encoding mutant and native subunits should be similar. Thus, it is unlikely that the N173Q mutation-induced reduction of mutant subunit expression was due to decreased *de novo* subunit synthesis but was caused most likely by degradation of subunits by ER-associated degradation, possibly due to impaired interactions with ER chaperones or subunit folding. Consistently, total levels of β2(N104Q/N173Q) and β2(N32Q/N173Q) subunits, double-Q subunits containing a mutation at the third glycosylation site, were also significantly lower (39 and 56% of native β2 subunit levels, respectively) than native subunit levels ($n = 5$; Fig. 2, *A* and *B*, *lanes 6* and *7*). Interestingly, total levels of β2(N104Q/N173Q), but not β2(N32Q/N173Q), subunits were even lower than those of β2(N173Q) subunits, suggesting a more important role of the second than the first glycosylation site for β2(N173Q) subunit stability. Although single mutation of the first or second glycosylation site did not reduce total levels of singly expressed subunits, total levels of double-Q mutant β2(N32Q/N104Q) subunits were significant lower than native β2 subunits, implying that the first and second glycosylation sites also played a role in subunit stability ($n = 4$; Fig. 2, *A* and *B*, *lanes 8*).

Asn and Gln may have very different effects on protein secondary structure. Asn is a potential breaker for a α-helix and β-strand secondary structures, but Gln is likely a former for the two secondary structures (34). Thus, it is possible that the Asn to Gln mutation *per se*, not the removal of the attached *N*-glycans, caused protein misfolding, faster degradation, and mobility shift. To examine this possibility, the Asn residue was mutated to Thr, Gly, or Pro, which is a former for a strand, a breaker for a helix, or breaker for both helix and strand, respectively (Fig. 2, *C* and *D*, *lanes 3–5*). If the changes caused by the N173Q mutation were due to perturbation of secondary structure by extending the β strand into the Cys-loop, then the N173T mutation would lead to similar changes, whereas the N173P mutations would not cause mobility shifts or decreases of total protein levels. The mutant β2(N173T) subunits migrated at the same molecular masses as the β2(N173G), β2(N173P), and β2(N173Q) subunits and were 2 kDa smaller than the native β2 subunits (Fig. 2*C*), which does not support the contention that the Asn to Gln mutation *per se* perturbed the secondary structure and caused the mobility shift. Likewise, the N173T, N173G, and N173P mutations caused significant decreases of total protein levels of mutant subunits relative to that of native β2 subunits but not to that of β2(N173Q) subunits, and 74, 76, and 77% of the native subunit levels of β2(N173T), β2(N173G), and β2(N173P) subunits, respectively, remained. Altogether, these results suggested that the Asn-173 site was the major glycosylation site determining the stability of β2 subunit expressed alone.

Glycosylation of Asn-104 Was Responsible for Full Surface Levels of Binary Receptors—Glycosylation also has been demonstrated to regulate surface targeting of Cys-loop receptors (4). To evaluate further how glycosylation of individual β2 subunit glycosylation sites regulated $GABA_A$ receptor biogenesis, mutant β2 subunits with single-, double-, or triple-Q mutations were coexpressed with α1 subunits (binary subunit coexpression), and surface levels of each subunit were measured using flow cytometry. FLAG epitopes were introduced into the α1 and β2 subunits to facilitate subunit measurement. To monitor surface levels of individual subunits, FLAG-tagged subunits were coexpressed with untagged partnering subunits. For instance, to evaluate the effects of the N32Q mutation, two transfection conditions were carried out, *i.e.* $\alpha1^{FLAG}\beta2(N32Q)$ and $\alpha1\beta2(N32Q)^{FLAG}$ subunit coexpression. Surface levels of the FLAG-tagged partnering α1 and FLAG-tagged mutant β2 subunits were then expressed as percentages of their respective "control" subunit levels, *i.e.* $\alpha1^{FLAG}$ subunits with $\alpha1^{FLAG}\beta2$ and $\beta2^{FLAG}$ subunits with $\alpha1\beta2^{FLAG}$ subunit coexpression.

Mutation of the second glycosylation site, N104Q, significantly reduced surface levels of both β2(N104Q) and partnering α1 subunits ($n = 5$), with only 57% of surface control α1 and 44% of surface control β2 subunits remaining. In contrast, mutation of the first, N32Q, or third, N173Q, glycosylation site did not alter α1 or β2 subunit surface levels (Fig. 3, *A* and *B*). The importance of the second glycosylation site for binary receptor surface expression was further supported by the double-Q mutant subunit, β2(N32Q/N173Q), as retaining only the second glycosylation site was sufficient to support full surface levels of both the β2(N32Q/N173Q) and the partnering α1 subunits (Fig. 3, *A* and *B*). With α1β2(N104Q/N173Q), α1β2(N32Q/N104Q), or α1β2(N32Q/N104Q/N173Q) subunit coexpression, surface α1 subunits were 24, 9, or 3%, and surface mutant β2 subunit levels were 15, 15, or 6% that of the corresponding control subunit levels, respectively. Although the surface levels of mutant β2 subunits or their corresponding partnering α1 subunits were not statistically different among these subunit coexpression conditions, they were all lower than the corresponding subunit surface levels with α1β2(N104Q) subunit coexpression, suggesting that mutating additional β2(N104Q) subunit glycosylation sites additively decreased receptor cell surface expression (Fig. 3, *A* and *B*).

Interplay of Receptor Cell Surface Targeting and Subunit Stability Determined Subunit Total Levels—Multiple steps are involved in efficient cell surface expression of $GABA_A$ receptors, including subunit expression, subunit-subunit oligomerization, pentameric assembly, and trafficking to the cell surface. It is interesting that although mutation of the third glycosylation site, Asn-173, caused instability of singly expressed subunits, it had no effect on binary receptor surface levels. Conversely, mutation of the second glycosylation site, Asn-104, which showed no effects on singly expressed subunit stability, significantly decreased binary receptor surface levels. Pentameric coassembly of α1 and β2 subunits can mutually increase total levels of both subunits (12, 31). It is possible that α1 subunits functioned as chaperones by coassembling with β2(N173Q) subunits and increasing their stability. In contrast, although β2(N104Q) subunits were not severely misfolded, coassembly of α1 and β2(N104Q) subunits might be inefficient, or pentamer stability might be decreased, both of which could lead to decreased total levels of mutant and partnering subunits. To test this hypothesis, total levels of partnering α1 and mutant β2 subunits were compared with those with control subunits (Fig. 4*A*). Consistent with surface levels, total

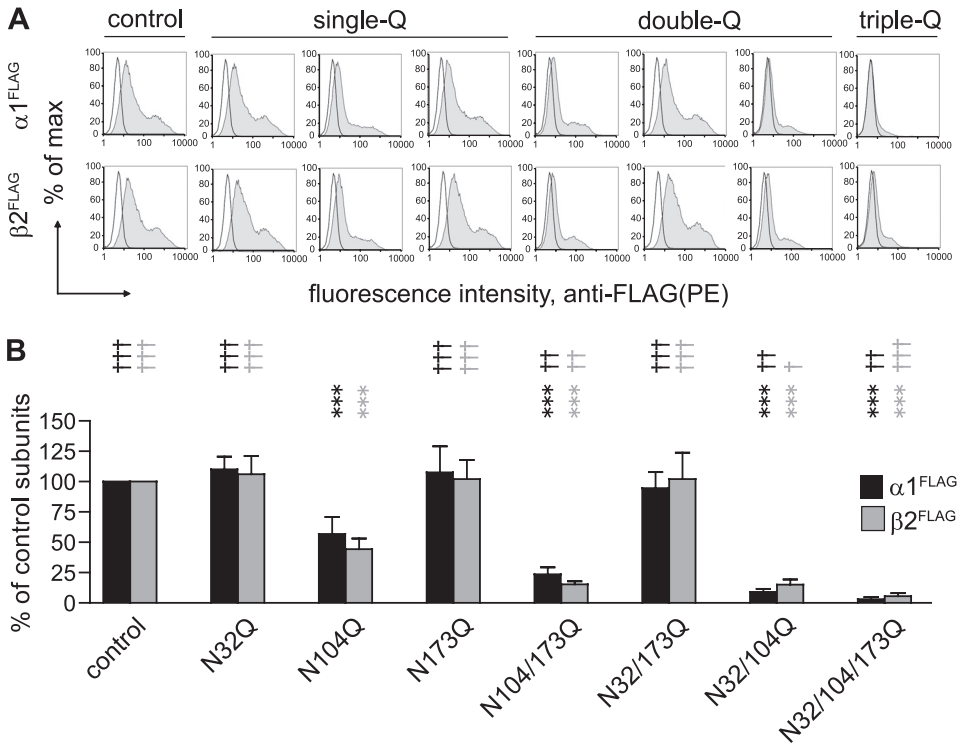

FIGURE 3. **Glycosylation of the second glycosylation site, Asn-104, was important for full cell surface levels of binary receptors.** *A*, cell surface expression levels of binary $\alpha1\beta2$ $GABA_A$ receptors containing mutated, glycosylation-deficient $\beta2$ subunits were analyzed using PE-conjugated monoclonal anti-FLAG antibody (M2 clone) and plotted as fluorescence intensity histograms. The *x* axis indicates the fluorescence intensity in arbitrary units (note the log scale), and the *y* axis indicates the percentage of the maximum cell count. Representative distribution obtained from mock-transfected cells (unfilled histogram) was overlaid with each experimental distribution (filled histograms). *Upper panels* indicate FLAG intensities on the cell surface from FLAG-tagged $\alpha1$ subunits ($\alpha1^{FLAG}$) coexpressed with non-tagged control or mutant $\beta2$ subunits. *Lower panels* indicate FLAG intensities on the cell surface from FLAG-tagged $\beta2$ subunits ($\beta2^{FLAG}$) with or without glycosylation mutations, coexpressed with non-tagged $\alpha1$ subunits. Similar to Fig. 2, the combinations of $\beta2$ subunit glycosylation site mutations for each column are indicated along the *bottom of the figure*. *B*, cell surface $\alpha1^{FLAG}$ (*black bars*) and $\beta2^{FLAG}$ (*gray bars*) subunit levels were quantified in each condition and expressed as percentages of cell surface levels of control subunits. Data are presented as the mean ± S.D. *** indicates $p < 0.001$ relative to control $\alpha1\beta2$ subunit coexpression. †, ††, and ††† indicate $p < 0.05$, $p < 0.01$, and $p < 0.001$, respectively, relative to $\alpha1\beta2$(N104Q) subunit coexpression.

levels of $\alpha1$ subunits coexpressed with mutant $\beta2$ subunits containing the intact Asn-104 glycosylation sequon ($\beta2$(N32Q), $\beta2$(N173Q), and $\beta2$(N32Q/N173Q) subunits) were not changed significantly (Fig. 4, *A* and *B*; *lanes 4*, *6*, and *8*), but total levels of $\alpha1$ subunits coexpressed with $\beta2$ subunits that had the mutation of residue Asn-104 ($\beta2$(N104Q), $\beta2$(N104Q/N173Q), $\beta2$(N32Q/N104Q), and $\beta2$(N32Q/N104Q/N173Q) subunits) were decreased significantly to 46, 31, 24, or 20% of control $\alpha1$ subunit levels, respectively ($n = 4$; Fig. 4, *A* and *B*, *lanes 5*, *7*, *9*, and *10*). In fact, all of the double- and triple-Q mutant subunits that included the N104Q mutation had $\alpha1$ subunit total expression levels that were not different from those in cells transfected with $\alpha1$ subunits alone ($n = 4$; Fig. 4, *A* and *C*, *lane 5*), which suggests that glycosylation of Asn-104 is important for assembly and/or stability of $\alpha1\beta2$ receptors. Interestingly, and unlike cell surface expression, except for $\beta2$(N32Q) subunits, total expression of all mutant $\beta2$ subunits was significantly reduced compared with control $\beta2$ subunits ($n = 5$), and only 42, 59, 10, 56, 12, and 4% of control $\beta2$ subunit total levels of $\beta2$(N104Q), $\beta2$(N173Q), $\beta2$(N104Q/N173Q), $\beta2$(N32Q/N173Q), $\beta2$(N32Q/N104Q), and $\beta2$(N32Q/N104Q/N173Q) subunits remained, respectively (Fig. 4*C*).

Of particular note, abolishing glycosylation of Asn-173 decreased total levels of mutant $\beta2$(N173Q) or $\beta2$(N32Q/N173Q) subunits but had no significant effects on total levels of partnering $\alpha1$ subunits or on $\alpha1\beta2$(N173Q) or $\alpha1\beta2$(N32Q/N173Q) receptor surface levels. Thus, although $\alpha1$ subunits could serve as chaperones to increase $\beta2$(N173Q) or $\beta2$(N32Q/N173Q) subunit levels, they could not fully restore them to control levels (Fig. 4*C*). Furthermore, this finding suggested that the forward trafficking machinery was saturated under control conditions and that the degradation machinery selectively degraded mutant subunits containing the N173Q mutation rather than their partnering subunits. Importantly, both mutant and partnering subunit total levels with coexpression of $\alpha1\beta2$(N104Q) subunits were significantly lower than those with coexpression of $\alpha1\beta2$(N173Q) subunits, suggesting that the N104Q mutation had stronger effects on decreasing binary subunit expression levels than the N173Q mutation.

Glycosylation of β2 Subunit Residue Asn-104 Was Important for Biogenic Steps in the ER—The reduced cell surface and total expression of $\beta2$(N104Q) subunits and partnering $\alpha1$ subunits could be due to altered receptor trafficking (decreased rate of forward trafficking and/or increased rate of endocytosis) or impaired biogenic steps that preceded forward trafficking beyond the ER (inefficient assembly and/or reduced stability of pentameric receptors in the ER). To distinguish between these two possibilities, forward trafficking and surface expression of receptors were blocked by incubating cells with brefeldin A, a drug that has been shown to collapse the Golgi apparatus, thus, arresting receptors in the ER (35, 36). If the reduction in cell surface and total protein expression of both $\beta2$(N104Q) and partnering $\alpha1$ subunits was due to altered $\alpha1\beta2$(N104Q) receptor trafficking, then blocking forward trafficking should abolish the difference in expression of control and mutant subunits and their corresponding partnering subunits. On the other hand, if the mutation affected biogenic steps earlier than forward trafficking beyond the ER, then expression of mutant and partnering subunit total levels should remain reduced compared with control subunits.

In cells treated with DMSO only, total levels of mutant $\beta2$(N104Q) subunits and their partnering $\alpha1$ subunits were lower relative to control $\alpha1$ and $\beta2$ subunit levels 24 h after transfection (Fig. 5, *A* and *B*, *top*). Quantitatively, total levels of

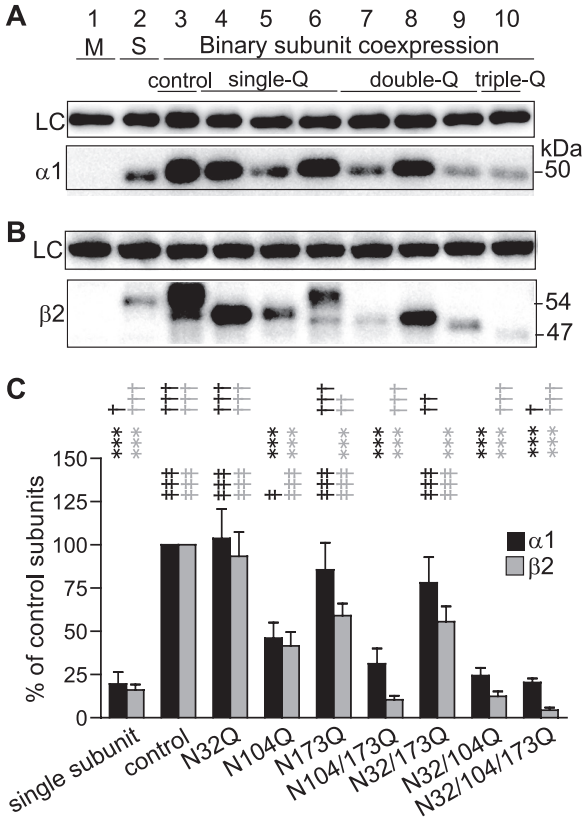

FIGURE 4. **Partnering α1 subunits increased total levels of the three single-Q and one of the double-Q β2 subunits.** *A*, proteins in the membrane fraction of HEK293T cells mock-transfected with empty vector (*M*, *lane 1*) or expressing single α1 subunit (*S*, *lane 2*) or binary α1β2 subunits were detected by Western blotting. Similar to Fig. 2, the combinations of β2 subunit glycosylation site mutations for each lane are indicated along the *bottom of the figure*. The *upper panel* presents the anti-Na^+/K^+-ATPase staining as a loading control (*LC*), and the *lower panel* presents the anti-α1 subunit staining. *B*, the loading order was the same as *A* except that *lane 2* was loaded with proteins from cells expressing single β2 subunits, and blots were stained using anti-β2 subunit cytoplasmic loop antibodies. *C*, total levels of α1 (*black bars*) and β2 (*gray bars*) subunits were quantified in each condition and expressed as percentages of total levels of corresponding control subunits. Data are presented as the mean ± S.D. ‡ and ‡‡‡ indicate $p < 0.05$ and $p < 0.001$, respectively, relative to subunit total levels of singly expressed α1 or β2 subunits. *** indicates $p < 0.001$ relative to the total levels of control α1 or β2 subunits with binary subunit expression. †, ††, and ††† indicate $p < 0.05$, $p < 0.01$, and $p < 0.001$, respectively, relative to the total level of α1 or β2(N104Q) subunits with α1β2(N104Q) subunit coexpression.

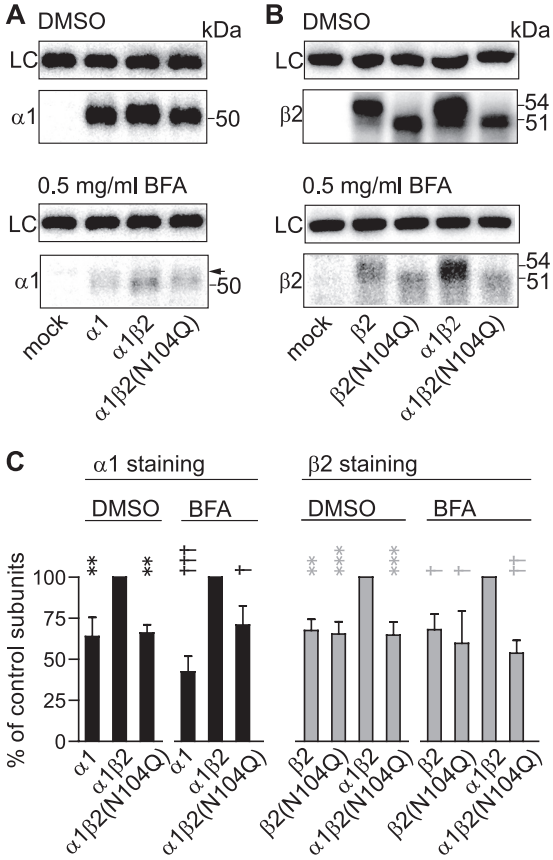

FIGURE 5. **Altered expression of β2(N104Q) subunits did not depend on changes in cellular forward trafficking beyond the ER.** *A*, cells expressing mock (empty vector transfection), α1 subunit alone, control α1β2 subunits or α1β2(N104Q) subunits were treated with either DMSO (*upper panels*) or 0.5 μg/ml brefeldin A (*BFA*; *lower panels*) 6 h after transfection and were harvested 24 h after transfection. Membrane fractions of cells from each transfection condition were then resolved using SDS-PAGE and immunoblotted with an anti-α1 subunit antibody. Na^+/K^+-ATPase was used as loading control (*LC*). The *arrowhead* indicates a nonspecific band sometimes detected by the anti-α1 subunit antibody. *B*, cells expressing mock, β2 subunit alone, β2(N104Q) subunit alone, control α1β2 subunits, or α1β2(N104Q) subunits were subjected to the same procedure described as *A* but were immunoblotted with anti-β2 subunit cytoplasmic loop antibodies. *C*, normalized total α1 subunit levels (*black bars*) and total β2 subunit levels (*gray bars*) with DMSO or brefeldin A treatment were plotted. Data are presented as the mean ± S.D. ** and *** indicate $p < 0.01$ and $p < 0.001$, respectively, relative to control α1β2 subunit coexpression with DMSO treatment. †, ††, and ††† indicate $p < 0.05$, $p < 0.01$, and $p < 0.001$, respectively, relative to control α1β2 subunit coexpression with BFA treatment.

α1 subunits expressed alone or with α1β2(N104Q) subunit coexpression were 64 and 66% that of control α1 subunits, respectively, and total levels of β2 and β2(N104Q) subunits expressed alone and of β2(N104Q) subunits with binary subunit coexpression were 68, 65, and 65% that of control β2 subunits, respectively (Fig. 5*C*).

Similar to DMSO treatment, total levels of control subunits remained significantly different from those of subunits expressed alone or from those with α1β2(N104Q) subunit coexpression in the presence of brefeldin A. Relative to control subunits coexpressed in cells treated with brefeldin A, 42% of α1 subunits expressed alone and 71% of α1 subunits coexpressed with β2(N104Q) subunits remained ($n = 3$; Fig. 5*C*), whereas 68% of β2 subunits expressed alone, 60% of β2(N104Q) subunits expressed alone, and 54% of β2(N104Q) subunits coexpressed with α1 subunits remained ($n = 3$; Fig. 5*C*). These results, thus, favored the argument that the second glycosylation site played a role in assembly and/or stability of pentameric receptors in the ER.

With Coexpression of α1 Subunits, Mutant β2(N104Q) Subunits Were Mainly Retained in the ER—After pentameric assembly, $GABA_A$ receptors are trafficked to the Golgi apparatus, where further processing of the *N*-glycans occurs and confers them with resistance to cleavage by endo H. Thus, if mutant subunits that contained the β2 subunit N104Q mutation impaired efficient $GABA_A$ receptor assembly and/or trafficking through the Golgi apparatus, β2(N104Q) subunits would have a reduced endo H-resistant fraction. To examine this hypothesis, endo H digestion patterns of membrane β2 subunits (including the surface and intracellular populations) with different combinations of mutations of the three *N*-linked glycosylation sites and with coexpression of α1 subunits were com-

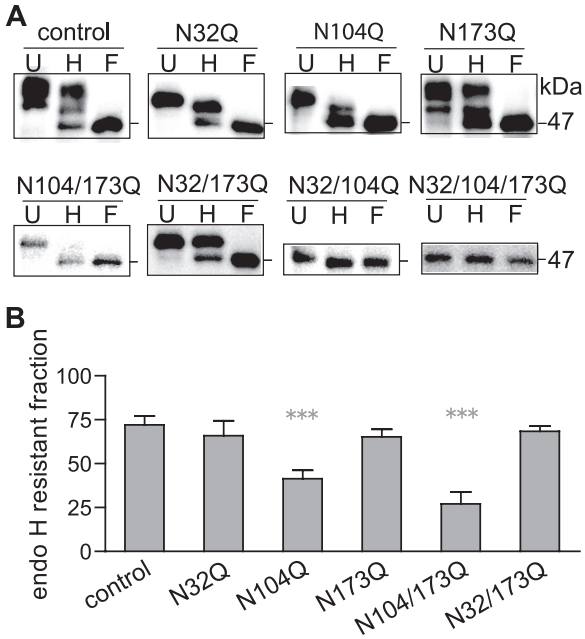

FIGURE 6. **With coexpression the mutant β2(N104Q) and partnering α1 subunits were mainly localized in the ER.** *A*, radioimmune precipitation assay buffer-extracted membrane proteins from HEK293T cells with coexpression of binary α1β2 subunits were undigested (*U*) or digested with endo H (*H*) or PNGase F (*F*) and then were subjected to SDS-PAGE. Resolved proteins were probed with anti-β2 subunit cytoplasmic loop antibodies. After endo H digestion, subunits with a molecular mass equal to that of subunits digested with PNGase F (47 kDa) were considered endo H-sensitive, whereas those with higher molecular masses were considered endo H-resistant. Specific combinations of glycosylation site mutations were annotated *above individual panels*. *B*, percentages of endo H-resistant β2 subunits that contained no mutations or N32Q, N104Q, N173Q, N104Q/N173Q, or N32Q/N173Q mutations with binary subunit coexpression were quantified by dividing the IDV of the endo H-resistant fraction by the summated IDV of endo H-resistant and -sensitive fractions. Data are presented as the mean ± S.D. *** indicates $p < 0.001$ relative to control β2 subunits.

pared with each other. Additionally, the undigested and PNGase F-digested conditions were also included in each experimental set to fully assess the endo H digestion effects on glycosylation-deficient mutants. Because the presence of endo H-resistant *N*-glycans attached to any one of the three β2 subunit *N*-linked glycosylation sites is sufficient to demonstrate the processing of *N*-glycans in the Golgi apparatus, the endo H-treated β2 subunits that migrated at molecular masses higher than that of subunits treated with PNGase F were classified as an endo H-resistant population.

Endo H and PNGase F digestion did not cause further mobility shifts of the triple-Q β2(N32Q/N104Q/N173Q) mutant subunits, which migrated at 47 kDa (Fig. 6*A*), supporting the conclusion that there were only three $GABA_A$ receptor β2 subunit *N*-linked glycosylation sites. The endo H-treated control β2 and β2(N173Q) subunits migrated mainly as three bands with two endo H-resistant populations at molecular masses of 53 and 50 kDa (Fig. 6*A*), which were 1 kDa smaller than the undigested control β2 subunits (54 and 51 kDa) but were the same as undigested β2(N173Q) subunits. Consistently, the endo H-digested β2(N32Q) or β2(N104Q) subunits migrated mainly as two bands with a single endo H-resistant population mainly migrating at 50 kDa (Fig. 6*A*), which was 1 kDa smaller than the undigested subunits, whereas the endo H-treated β2(N104Q/N173Q) or β2(N32Q/N173Q) subunits showed a single endo H-resistant band migrated at 50 kDa, which was the same as the undigested subunits.

The endo H-resistant fraction of each mutant β2 subunit was also calculated and expressed as the percentage of the total protein levels of each condition (Fig. 6*B*). Because of the absence of endo H-resistant populations of β2(N32Q/N104Q) and β2(N32Q/N104Q/N173Q) subunits, they were excluded from endo H-resistant fraction analysis. In agreement with their comparable surface levels, the endo H-resistant populations of control β2 and mutants β2(N32Q), β2(N173Q), and β2(N32Q/N173Q) subunits were 72, 66, 65, or 68% of total subunit levels, respectively, and were not significantly different from each other (Fig. 6*B*). Likewise, the lower surface levels of α1β2(N104Q) and α1β2(N104Q/N173Q) receptors correlated with significantly smaller endo H-resistant populations of β2(N104Q) and β2(N104Q/N173Q) subunits, which were 42 and 27% of total subunit levels, respectively (Fig. 6*B*). Thus, our observations suggested that *N*-glycans attached to β2 subunit Asn-173 sites in receptor complexes passing through Golgi apparatus were not conferred with endo H resistance. Furthermore, abolishing glycosylation of residue Asn-104 increased the ER localization of the remaining mutant subunits.

High Mannose N-Glycans Are Abundant at Asn-173 Sites of Surface β2 Subunit—It is worth emphasizing that *N*-glycans attached to the Asn-173 site were different from those attached to the other two sites as they remained endo H-sensitive as the receptor passed through the Golgi apparatus. Thus, to further investigate the basis for the distinct property of *N*-glycans attached to the Asn-173 site, *N*-glycans of the surface β2 subunits were subjected to glycomic profiling and were compared with those of surface β2(N32Q) and β2(N173Q) subunits. To avoid purifying *N*-glycans contributed by the α1 subunit and to facilitate protein purification, the $\alpha1(\text{loop}\Delta)^{\text{FLAG}}$ subunit, a FLAG-tagged α1 subunit with 52 amino acids deleted from the N-terminal half of cytoplasmic TM3-TM4 loop, was coexpressed with β2 or glycosylation-deficient β2 subunits. The endoglycosidase digestion demonstrated that the $\alpha1(\text{loop}\Delta)^{\text{FLAG}}$ subunit did not affect the gross molecular masses of cell surface β2, β2(N32Q), β2(N104Q), or β2(N173Q) subunits before or after the endo H or PNGase F treatments (Fig. 7*A*).

Glycomic analyses revealed high mannose and complex *N*-glycans from each sample of surface β2, β2(N32Q), and β2(N173Q) subunits. Structures of *N*-glycans were assigned from compositional information inferred from the mass over charge (*m*/*z*) values and taking into account biosynthetic considerations. The highest quality *N*-glycan data were obtained from surface β2(N32Q) subunits (Fig. 7*B*). The most abundant β2(N32Q) subunit *N*-glycan class were high mannose forms with compositions of 0 to 1 glucoses (Glc), 7–9 mannoses (Man), and 2 *N*-acetylglucosamines (GlcNAc), $Glc_{0-1}Man_{7-9}GlcNAc_2$, and their *m*/*z* values were 1988, 2192, 2396, and 2600. Furthermore, complex glycans were present with compositions that were consistent with bi-antennary structures with varying levels of antennal sialylation and fucosylation. Surface β2 subunit *N*-glycans were comparable with those found in surface β2(N32Q) subunits, and the two peaks

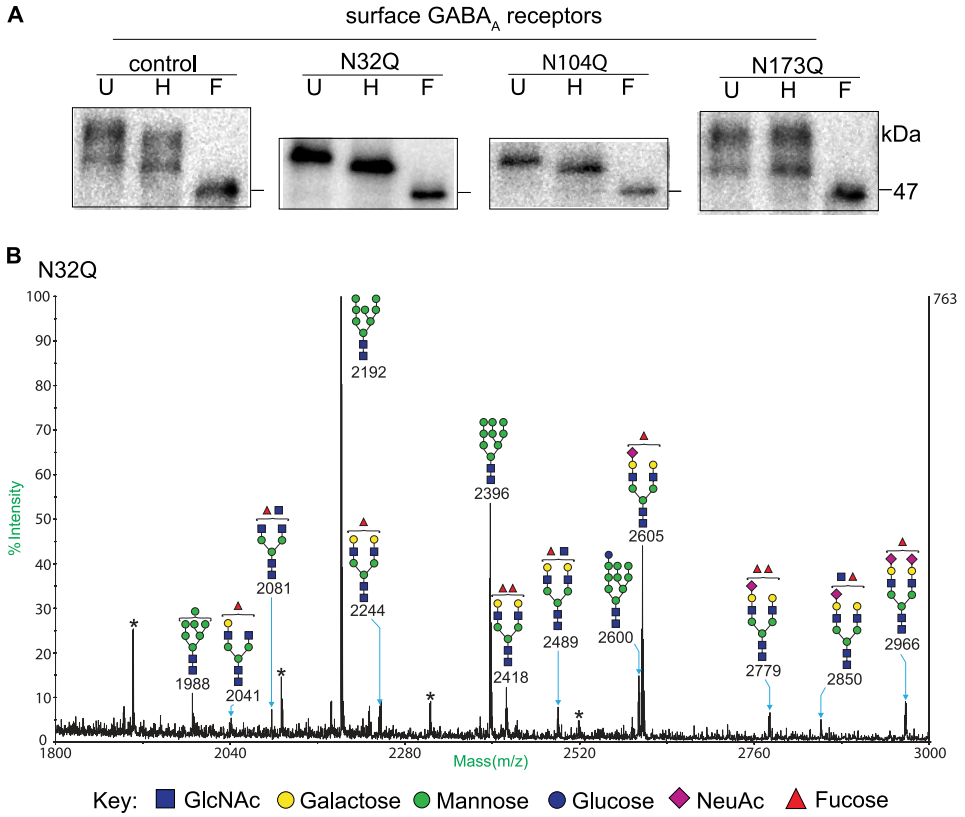

FIGURE 7. ***N*-Glycans attached to the Asn-173 site of surface α1β2 receptors were endo H-sensitive in high mannose forms.** *A*, surface proteins of HEK cells coexpressing α1β2, α1β2(N32Q), α1β2(N104Q), or α1β2(N173Q) subunits were biotinylated and pulled down with streptavidin beads. The purified proteins were undigested (*U*) or digested with endo H (*H*) or PNGase F (*F*). Surface proteins were then resolved by SDS-PAGE and probed with anti-β2 subunit antibodies. *B*, surface proteins of HEK cells with α1(loopΔ)^{FLAG}β2(N32Q) subunit coexpression, where the α1(loopΔ)^{FLAG} subunit was a FLAG-tagged α1 subunit with half of its cytoplasmic loop truncated, were biotinylated and subjected to sequential anti-FLAG immunoprecipitation and streptavidin-bead pulldown and then resolved by SDS-PAGE. The band corresponding to the β2(N32Q) subunits was excised and subjected to glycomic profiling (see "Experimental Procedures") The mass spectrum of permethylated *N*-glycans is presented, and ions are $[M+Na]^+$. The symbol presentation of *N*-glycans is based on the Consortium for Functional Glycomics guidelines. A structure containing monosaccharides *outside the bracket* suggests potential structural heterogeneity of the peak. * indicates hexose polymeric contamination.

with highest intensities also represented $Man_8GlcNAc_2$ (*m/z* 2192) and $Man_9GlcNAc_2$ (*m/z* 2396) *N*-glycans (supplemental Fig. 3). In contrast, the profile of *N*-glycans attached to surface β2(N173Q) subunits was different from that of the surface β2 or β2(N32Q) subunits (supplemental Fig. 3). The most abundant *N*-glycans of the surface β2(N173Q) subunits were the complex forms (*m/z* 2041, 2244, 2418, 2489, and 2605), and levels of the high mannose forms (*m/z* 1988, 2192, and 2396) attached to the subunits were reduced. Thus, glycomic profiling of the surface fractions of β2, β2(N32Q), and β2(N173Q) subunits suggested that the most abundant class of *N*-glycans attached to the Asn-173 site were high mannose forms whose cleavage by endo H would be consistent with the band shifts observed in Fig. 7*A*. Together, the endoglycosidase digestion and glycomic profiling of the surface β2, β2(N32Q), and β2(N173Q) subunits indicted that the majority of *N*-glycans attached to the Asn-173 site were protected from *N*-glycan processing in the Golgi apparatus.

Mutation of β2 Subunit Glycosylation Sites Decreased Peak Current Amplitudes of Binary α1β2 Receptors—Previous studies suggest that glycosylation of Cys-loop receptors affects channel properties (4, 9, 37, 38). To evaluate how β2 subunit glycosylation sites regulate GABA$_A$ receptor channel function, 1 mM or 1 μM GABA was applied using a rapid exchange system to lifted HEK293T cells coexpressing α1β2, α1β2(N32Q), α1β2(N104Q), or α1β2(N173Q) subunits. Measuring peak current amplitudes evoked by 1 mM GABA revealed that β2 subunit with an N32Q, N104Q, or N173Q mutation reduced the α1β2 receptor peak current amplitudes from 2514 to 952, 49, and 321 pA, respectively (Fig. 8, *A* and *B*). Given that surface levels of both subunits with α1β2(N32Q) or α1β2(N173Q) subunit coexpression were comparable with control subunits, the observation suggested that receptor function was impaired by mutation of the first or third glycosylation site. To explore this possibility more extensively, we performed a detailed kinetic analysis of GABA-evoked currents from wild-type and mutant subunits expressed as binary α1β2 receptors. Currents of α1β2(N104Q) receptors were omitted due to small current amplitudes. GABA potency was assessed by measuring the peak current amplitudes evoked by 1 μM GABA normalized to the peak current evoked by 1 mM GABA in the same cell. Normalized α1β2, α1β2(N32Q), or α1β2(N173Q) receptor peak current amplitudes evoked by 1 μM GABA were 15, 18, and 5% (Fig. 8*B*, Table 2). The responses of mutant α1β2(N173Q) receptors evoked by 1 μM GABA application were significantly smaller than those from α1β2 and α1β2(N32Q) receptors, suggesting differences in agonist potency to activate these receptors. The macroscopic current kinetic properties (desensitization and deactivation time courses) of currents evoked by 1 mM GABA were also analyzed and compared (see "Experimental Procedures"). Receptor desensitization was assessed as the magnitude of the residual relative to peak currents at the ends of 1 mM GABA applications. We found that the residual currents obtained from α1β2, α1β2(N32Q), or α1β2(N173Q) receptors were 20, 20, and 37% of the peak currents, respectively. Although not statistically significant, this result suggested that α1β2(N173Q), but not α1β2(N32Q), receptor currents desensitized more slowly or less extensively than control currents (Fig. 8*C*, *left*; Table 2). The weighted deactivation time constants of control α1β2, α1β2(N32Q) and α1β2(N173Q) receptor currents were 125, 113, and 73 ms, respectively (Fig. 8*C*, *right*; Table 2). The last was significantly smaller than the first two, which were not statistically different from each other.

Taken together, $\alpha1\beta2$(N173Q) receptors were less sensitive to low levels of GABA and deactivated more rapidly than either wild-type or $\alpha1\beta2$(N32Q) receptors, suggesting that the N173Q and N32Q mutations affected channel function differently. It is worth noting that the currents recorded from $\alpha1\beta2$(N104Q) receptors (~2% of peak current amplitudes of control receptor currents) were 1 order of magnitude smaller than the relative receptor surface levels, which were about 50% of control receptor surface levels, suggesting that the second glycosylation mutation also affected channel properties.

Elimination of Any of the β2 Subunit Glycosylation Sites Altered Single Channel Gating of Binary α1β2 Receptors—To investigate further how mutations of β2 subunit glycosylation sites affected macroscopic current kinetics, single channel properties of the binary receptors containing one of the single-Q mutations were further compared with control receptors using cell-attached single-channel recording (Fig. 9). Amplitude histograms revealed similar single channel current amplitudes for control $\alpha1\beta2$ and mutant $\alpha1\beta2$(N32Q), $\alpha1\beta2$(N104Q), and $\alpha1\beta2$(N173Q) receptors (Table 2), suggesting that single-Q mutations did not affect single-channel conductance. However, the mean open time of control channels was 2.24 ms, which was about 2 times longer than those of single-Q mutant channels, 0.97, 0.83, and 1.06 ms for $\alpha1\beta2$(N32Q), $\alpha1\beta2$(N104Q), or $\alpha1\beta2$(N173Q) receptors, respectively (n = 3–6; Table 2). To determine the basis for the reduction in mean channel open time produced by the glycosylation site mutations, we analyzed open duration histograms for control and mutant single channel currents evoked by 1 mM GABA. Each open duration histogram for single channel currents evoked from the four different receptors was fitted best with a sum of two exponential functions (Fig. 9*B*). Although time con-

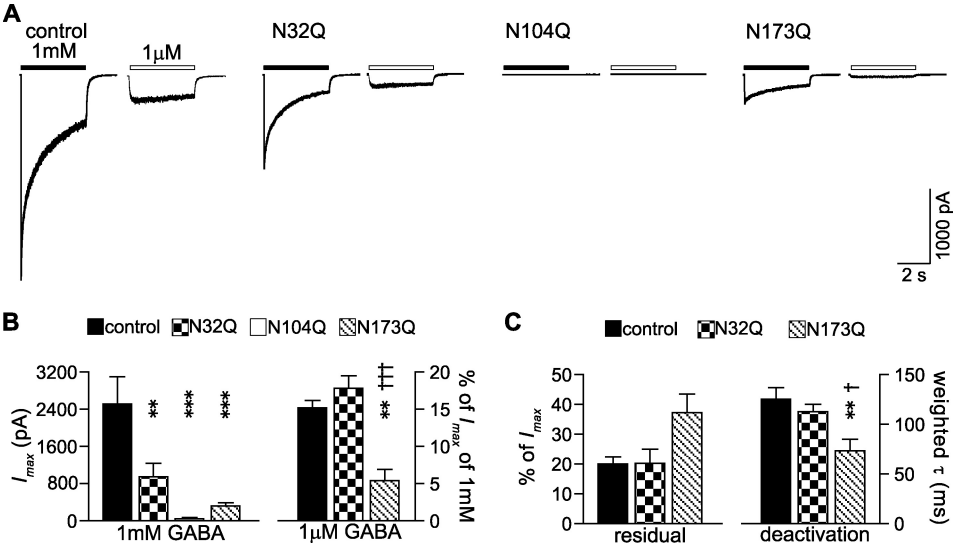

FIGURE 8. **Glycosylation site mutations decreased peak current amplitudes and altered macroscopic current kinetics.** *A*, currents were obtained from cells coexpressing control $\alpha1\beta2$, $\alpha1\beta2$(N32Q), $\alpha1\beta2$(N104Q), or $\alpha1\beta2$(N173Q) subunits in response to rapid application of 4 s pulse of 1 mM or 1 μM GABA. The duration of GABA application was indicated by a *black* (1 mM GABA) or *white* (1 μM GABA) *bar above each current trace*. Cells were voltage-clamped at −20 mV. *B*, means of peak current amplitudes (I_{max}) of each control $\alpha1\beta2$ (*black bars*), $\alpha1\beta2$(N32Q) (*checkered bars*), $\alpha1\beta2$(N104Q) (*white bars*), or $\alpha1\beta2$(N173Q) (*hatched bars*) receptors evoked by 1 mM GABA or by 1 μM GABA (expressed as % of I_{max}) were plotted. *C*, residual currents at the end of the 4-s application of 1 mM GABA (expressed as % of I_{max}) and their weighted deactivation time constants (τs) of $\alpha1\beta2$ (*black bars*), $\alpha1\beta2$(N32Q) (*checkered bars*), or $\alpha1\beta2$(N173Q) (*hatched bars*) receptors were plotted. The currents evoked by 1 μM GABA and the kinetic properties of macroscopic currents evoked by 1 mM GABA from $\alpha1\beta2$(N104Q) receptors were omitted from analyses due to low current amplitudes. Data are presented as the mean ± S.E. ** and *** indicate $p < 0.01$ and $p < 0.001$, respectively, relative to control $\alpha1\beta2$ subunit coexpression. † and ††† indicate $p < 0.05$ and $p < 0001$, respectively, relative to $\alpha1\beta2$(N32Q) subunit coexpression.

TABLE 2

Effects of β2 subunit glycosylation site mutations on α1β2 receptor channel function

Kinetic parameters of whole-cell currents were obtained from macroscopic currents recorded from lifted cells, which were voltage-clamped at −20 mV and applied with 1 mM GABA or 1 μM GABA for 4 s. I_{max}, $I_{residual}$, and $\tau_{deactivation}$ refer to peak current amplitudes, residual current amplitudes at the end of GABA applications, and weighted deactivation time constants, respectively. Kinetic parameters of single-channel currents in attached-cell patches held at +80 mV with 1 mM GABA in the glass-electrodes were obtained. The *i* refers to current amplitudes of single-channel currents; τ and A refer to the time constants and fractions of the two exponential components (short and long), which best represent the distributions of the single-channel openings. Values reported are the mean ± S.E. NA refers to not available.

	Control β2	β2(N32Q)	β2(N104Q)	β2(N173Q)
Whole-cell currents[a]				
1 mM GABA				
$I_{max[1\ mM]}$ (pA)	2514 ± 586	952 ± 287[a]	49 ± 2[b]	321 ± 73[b]
$I_{residual}$ (% of $I_{max[1mM]}$)	20.0 ± 2.4	20.3 ± 4.7	NA	37.3 ± 6.2
$\tau_{deactivation}$	125.3 ± 11.9	112.7 ± 7.5	NA	73.3 ± 11.6[a,c]
1 μM GABA				
$I_{max[1\ \mu M]}$ (% of $I_{max[1\ mM]}$)	15.2 ± 1.0	17.9 ± 1.7	NA	5.4 ± 1.5[a,d]
Single-channel currents[b]				
i (pA)	0.92 ± 0.04	0.95 ± 0.04	0.90 ± 0.05	0.91 ± 0.02
Mean open time (ms)	2.24 ± 0.06	0.97 ± 0.07[b]	0.83 ± 0.10[b]	1.06 ± 0.09[b]
τt_{short} (ms)	0.82 ± 0.15	0.68 ± 0.08	0.58 ± 0.10	0.74 ± 0.08
τ_{long} (ms)	2.53 ± 0.53	2.39 ± 0.55	1.75 ± 0.14	1.57 ± 0.13
A_{short} (%)	85.47 ± 2.67	98.70 ± 0.64[e]	99.57 ± 0.03[a]	96.12 ± 2.41[e]
A_{long} (%)	14.53 ± 2.67	1.30 ± 0.64[e]	0.43 ± 0.03[a]	3.88 ± 2.41[e]

[a] $p < 0.01$ relative to control conditions.
[b] $p < 0.001$ relative to control conditions.
[c] $p < 0.05$ relative to $\alpha1\beta2$(N32Q) subunit coexpression.
[d] $p < 0.001$ relative to $\alpha1\beta2$(N32Q) subunit coexpression.
[e] $p < 0.05$ relative to control conditions.

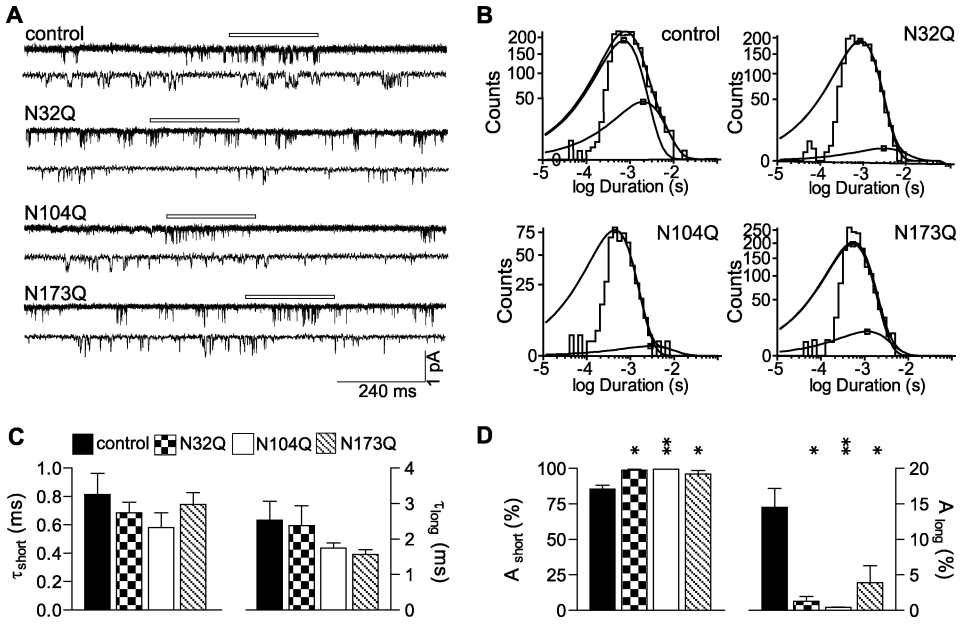

FIGURE 9. **Glycosylation site mutations decreased mean single channel open time by decreasing the occupancy of long-duration open states.** *A*, representative steady-state single-channel currents evoked by 1 mM GABA were obtained from cells coexpressing control $\alpha1\beta2$ (first set), $\alpha1\beta2$(N32Q) (second set), $\alpha1\beta2$(N104Q) (third set), or $\alpha1\beta2$(N173Q) (fourth set) subunits. The *upper trace of each set* was a continuous 1-s recording, and the *lower trace* was a continuous 240-ms recording expanded from a portion of the upper trace (*white bar*). Cells were voltage-clamped at +80 mV. Openings were downward. *B*, representative open duration frequency histograms of single-channel currents from control $\alpha1\beta2$ (*upper left*), $\alpha1\beta2$(N32Q) (*upper right*), $\alpha1\beta2$(N104Q) (*lower left*), or $\alpha1\beta2$(N173Q) (*lower right*) receptors are presented. Each histogram was fitted best with two exponential components (short and long). *C*, means of the open durations of the short and long open states of control $\alpha1\beta2$ (*black bars*), $\alpha1\beta2$(N32Q) (*checkered bars*), $\alpha1\beta2$(N104Q) (*white bars*), or $\alpha1\beta2$(N173Q) (*hatched bars*) receptors were plotted. *D*, relative proportions of the short and long open states of control $\alpha1\beta2$ (*black bars*), $\alpha1\beta2$(N32Q) (*checkered bars*), $\alpha1\beta2$(N104Q) (*white bars*), or $\alpha1\beta2$(N173Q) (*hatched bars*) receptors were plotted. Data are presented as the mean ± S.E. * and ** indicate $p < 0.05$ and $p < 0.01$, respectively, relative to control $\alpha1\beta2$ subunit coexpression.

stants of the short and long open states were similar (Fig. 9*C*), the relative proportion of the long open states of single-Q mutant channels was significantly decreased ($n = 3–6$) (Fig. 9*D*). For $\alpha1\beta2$, $\alpha1\beta2$(N32Q), $\alpha1\beta2$(N104Q), and $\alpha1\beta2$(N173Q) channels, relative proportions of the long open states were 14.5, 1.3, 0.4, and 3.9%, respectively (Fig. 9*D*; Table 2). Thus, the reduction of mean channel open time produced by the glycosylation site mutations was due to a shift in proportion of long open states to short open states and not due to destabilization of long or short open states, and the reduction of macroscopic currents was due to a combination of reduced cell surface expression and reduced mean open time of single channel currents.

DISCUSSION

N-Glycans Attached to the β2 Subunit Asn-173 Site May Interact with the Outer Sheet of the Same Subunits—It is intriguing that the N173Q mutation caused less mobility shift than the shift caused by a mutation of either the other two sites when expressed alone or coexpressed with $\alpha1$ subunits. This unique phenomenon raised the question of whether or not the mobility shift was due to removal of *N*-glycans from the Asn-173 site. The endo H-resistant $\beta2$ subunits retaining an Asn-173 site, but not those containing a mutation of Asn-173 site, specifically showed a 1-kDa shift by endo H treatments relative to undigested conditions. Thus, the N173Q mutation-independent 1-kDa shifts strongly supported the conclusion that removal of Asn-173 site *N*-glycans causes only a 1-kDa shift (Figs. 6*A* and 7*A*). Furthermore, amino acid frequency analysis of Asn-173 equivalent sites of the whole human Cys-loop receptor superfamily (45 homologous subunits) suggested that the N173Q mutation *per se* may not perturb secondary structure. First, the nicotinic acetylcholine receptor $\alpha9$ subunit has a Gln, not an Asn, at the Asn-173 equivalent side, indicating that the Asn to Gln substitution is tolerated by natural selection. Second, after the Asn residue, which occurs in 23 subunits of the whole superfamily, the most frequent amino acids occupying the Asn-173 equivalent site are Thr, Ala, or Ser, which occur in 7, 6, and 5 subunits, respectively. Despite Asn being a breaker for α helixes or β strands, Thr and Ala residues favor β strand and α helix formation, respectively (34). Thus, it is unlikely that a specific secondary structure must be conserved at this position. In agreement with the prediction, substitutions of the Asn at the 173 site with Gln, Thr, Pro, or Gly to favor α helix, β strand, or loop formation showed no significant differences in mobility shifts or subunit total level decreases. Our homology model suggested that the most abundant *N*-glycan ($Man_8GlcNAc_2$) attached to the Asn-173 site of each $\beta2$ subunit detected in glycomic analyses could make non-covalent interactions with the outer sheet of the same subunit and could play an important role in stabilizing the β-sandwich fold. Thus, removing the *N*-glycan from the Asn-173 site before receptor assembly may cause misfolding of $\beta2$ subunits, which in turn decreases the total $\beta2$ subunit level and causes less mobility shift than removing *N*-glycans from the Asn-32 or Asn-104 sites.

N-Glycans Attached to the β2 Subunit Asn-104 Site May Interact with the Inner Sheet of the Adjacent Subunits—Because the N104Q mutation still decreased $\beta2$(N104Q) and partnering $\alpha1$ subunit levels when forward trafficking beyond the ER was blocked by brefeldin A, glycosylation of Asn-104 was implicated in biogenic steps in the ER. Furthermore, consistent with a previous report that swapping out a five-amino acid motif including a Asn-104 equivalent glycosylation site from $\beta3$ subunits decreased $\beta3$ subunit levels but did not prevent oligomerization of $\beta3$ and $\alpha1$ subunits (39), co-immunoprecipitation efficiency between $\alpha1$ and mutant $\beta2$(N104Q) subunits was not different from that between control subunits (data not shown). Thus, glycosylation of Asn-104 was more likely to play a role in the later steps of pentameric assembly and/or receptor stability in the ER. Accordingly, we propose that *N*-glycans attached to

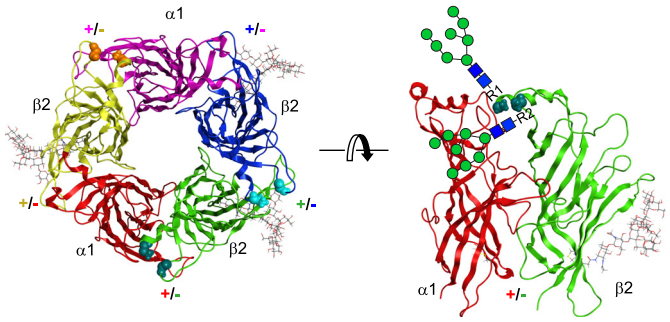

FIGURE 10. **$GABA_A$ receptor β2 subunit *N*-glycans can interact with intra-subunit amino acids and may also interact with those of adjacent subunits.** The *left panel* shows a top view of the pentameric extracellular model of the α1β2 $GABA_A$ receptor. The extracellular models of subunits were assembled in the counterclockwise order of α1-β2-β2-α1-β2 and in the color of *red-green-blue-pink-yellow* using the pentameric acetylcholine-binding protein as a scaffold. Furthermore, the atomic structure of the *N*-glycan, $Man_8GlcNAc_2$, which is available in the mouse nACh receptor α1 subunit template, was attached to each of the Asn-173 sites in the three β2 subunits (see "Experimental Procedures"). Space-filling residue backbones of the β2 subunit Asn-32 and Asn-104 at the very beginning and the L3 loop of subunits, respectively, are presented. They were colored in *teal*, *cyan*, and *orange* and belong to β2 subunits in *green*, *blue*, and *yellow*, respectively. At subunit interfaces, the plus or minus side of a given subunit was annotated as + or −, respectively, according to the subunit color codes. The *right panel* shows a side view of the α1/β2 subunit interface. The side chains of the Asn-173 glycosylation site and the Cys-160 and Cys-174 residues, which form signature disulfide bonds, are shown. Due to the absence of an atomic detail structure, two schematic $Man_8GlcNAc_2$ *N*-glycans, which are potential *N*-glycans attached to the fully assembled pentamers in the ER, were attached to the R1 or R2, which represent the side chain of Asn-32 or Asn-104, respectively.

the Asn-104 site in a way similar to the *N*-glycans of the Asn-173 site and make stabilizing contacts with adjacent subunits and/or chaperones at later stages of receptor assembly (Fig. 10).

Based on our homology model, the first and second β2 subunit glycosylation sites, Asn-32 and Asn-104, which are located one amino acid before the α1 helix and in the loop L3, respectively, are spatially close to each other near the top of the subunit (Fig. 10). Supporting this prediction, both N32Q and N104Q mutations decreased the affinity of a monoclonal antibody against the N-terminal epitope containing the Asn-32 residue (supplemental Fig. 1). Interestingly, glycosylation of Asn-32 was not sufficient to support control level cell surface expression in the absence of glycosylation of Asn-104 regardless of the spatial adjacency between the two glycosylation sites.

Glycosylation of β2 Subunits Regulated Binary Receptor Channel Gating—Available atomic structures and homology models suggest that each Cys-loop receptor subunit has "plus" and "minus" sides that contact adjacent subunits. For a subunit N-terminal domain, the plus side is composed of loops, whereas the minus side is composed mainly of β strands (22, 40). Specifically, loops (L5, L8, and L10, which conventionally are named loop A, B, and C, respectively) on the plus side of a subunit, together with β strands (β2, β5, β6) and a loop (L9) on the minus side of the adjacent subunit form the ligand binding pocket (22). It has been inferred that ligand binding and channel opening are coupled by conformational changes either mainly of α subunits of nicotinic acetylcholine receptors, (41) or globally involve all subunits (42, 43). Both mechanisms, however, suggest conformational changes of the whole extracellular domain of acetylcholine receptor α-type subunits (equivalent to $GABA_A$ receptor β subunits). Additionally, the pin-into-socket mechanism predicts that ligand binding-induced conformational changes release the anticlockwise rotation of the whole inner β sheet of the acetylcholine receptor α subunit and move L3 loop and the α1 helix elements of the subunit closer (40). In support of these predictions, our results suggested that glycosylation of Asn-32 before the α1 helix and Asn-104 in the L3 loop was required for proper channel gating. Furthermore, despite the Asn-173 site and its *N*-glycan being spatially distant from the Asn-32 and Asn-104 sites, they also regulated channel function. Interactions between L2, L7 (Cys-loop), and the TM2-TM3 linker have been implicated in coupling ligand binding to channel gating (44–46). Because the Asn-173 *N*-glycan could interact with the outer sheet of the β2 subunit including loop C, the interaction might play a role in transmitting the conformational change wave.

We demonstrated that the N173Q mutation resulted in decreased peak current amplitude by decreasing the relative proportion of long openings, thus, decreasing mean open time. This observation is different from the finding that mutations of the equivalent sites in non-α subunits of nicotinic acetylcholine receptors affected conductance, but not mean open time, of single channels (37). On the other hand, a conserved valine residue in the signature Cys-loops, which is shared by all human acetylcholine receptor subunits, asymmetrically regulated receptor gating (only showing effects in α and δ subunits of acetylcholine receptors) by decreasing the fraction of receptors that enter into long open states (47). Thus, it is possible that only glycosylation in Cys-loops of α type subunits of acetylcholine receptors (equivalent to β type subunits of $GABA_A$ receptors) and equivalent subunits of other Cys-loop superfamily receptors has effects on channel gating.

We also found that the N173Q mutation significantly decreased deactivation time constants of binary receptor macroscopic currents. Mutation of the Asn-173 equivalent glycosylation site of 5-HT_3 A subunit receptors has been shown to decrease maximal channel function without affecting antagonist binding affinity (4). Thus, the decrease in current amplitude may not be caused by a decrease in GABA affinity but by a decrease in $GABA_A$ receptor channel function. However, we could not rule out the possibility that the N173Q mutation slightly deformed the binding pocket and destabilized GABA-binding as *N*-glycans at the Asn-173 site might interact with L10 (loop C), which moves drastically after ligand binding.

Mutations around Glycosylation Sequons May Affect Glycosylation Efficiency—Our data suggested that a lack of glycosylation of Asn-32 impaired channel function of α1β2(N32Q) receptors without decreasing surface levels. In addition, our results suggested that glycosylation efficiency of Asn-32 was not as high as glycosylation of Asn-104 or Asn-173 due to the weaker sequon for *N*-glycan conjugation. Analysis of surface-biotinylated $GABA_A$ receptors from HEK cells coexpressing control α1β2 subunits revealed that surface β2 subunits mainly migrated at two molecular masses. This observation suggested that cell surface receptors in control conditions contained some β2 subunits that were not glycosylated at the first glycosylation site, and $GABA_A$ receptor currents could be increased further if glycosylation efficiency of Asn-32 were increased. Thus, weaker

sequons may serve as an element that could be regulated to fine tune $GABA_A$ receptor responses.

$GABA_A$ receptor N-terminal domains of human, rat, and mouse β subunits are highly homologous, and it is reasonable to apply observations from the N-terminal domain of one β subunit subtype to other subtypes. A mutation, G32R, that is one amino acid N-terminal to the first glycosylation site of $GABA_A$ receptor β3 subunits and is associated with childhood absence epilepsy has been demonstrated to reduce peak current amplitudes of α1β3(G32R)γ2S receptor channels (48). The G32R mutation may affect glycosylation efficiency of β3 N33 and in turn potentially could affect channel function. It remains to be determined whether or not the β3 subunit G32R mutation affects the *N*-linked glycosylation as well as how the mutation impaired channel function.

Acknowledgments—We thank Dr. Martin Gallagher for critical reading of this manuscript and Yueli Zhang, Ningning Hu, and Wangzhen Shen for technical assistance. We are also grateful to the Center for Structural Biology at Vanderbilt University for software usage.

REFERENCES

1. Marklová, E., and Albahri, Z. (2007) *Clin. Chim. Acta* **385,** 6–20
2. Connolly, C. N., Krishek, B. J., McDonald, B. J., Smart, T. G., and Moss, S. J. (1996) *J. Biol. Chem.* **271,** 89–96
3. Merlie, J. P., Sebbane, R., Tzartos, S., and Lindstrom, J. (1982) *J. Biol. Chem.* **257,** 2694–2701
4. Quirk, P. L., Rao, S., Roth, B. L., and Siegel, R. E. (2004) *J. Neurosci. Res.* **77,** 498–506
5. McKernan, R. M., and Whiting, P. J. (1996) *Trends Neurosci.* **19,** 139–143
6. Mortensen, M., and Smart, T. G. (2006) *J. Physiol.* **577,** 841–856
7. Pless, D. D., and Lennarz, W. J. (1977) *Proc. Natl. Acad. Sci. U.S.A.* **74,** 134–138
8. Corpet, F. (1988) *Nucleic Acids Res.* **16,** 10881–10890
9. Buller, A. L., Hastings, G. A., Kirkness, E. F., and Fraser, C. M. (1994) *Mol. Pharmacol.* **46,** 858–865
10. Chen, D., Dang, H., and Patrick, J. W. (1998) *J. Neurochem.* **70,** 349–357
11. Dellisanti, C. D., Yao, Y., Stroud, J. C., Wang, Z. Z., and Chen, L. (2007) *Nat. Neurosci.* **10,** 953–962
12. Lo, W. Y., Botzolakis, E. J., Tang, X., and Macdonald, R. L. (2008) *J. Biol. Chem.* **283,** 29740–29752
13. Angelotti, T. P., and Macdonald, R. L. (1993) *J. Neurosci.* **13,** 1429–1440
14. Greenfield, L. J., Jr., Sun, F., Neelands, T. R., Burgard, E. C., Donnelly, J. L., and MacDonald, R. L. (1997) *Neuropharmacology* **36,** 63–73
15. Jang-Lee, J., North, S. J., Sutton-Smith, M., Goldberg, D., Panico, M., Morris, H., Haslam, S., and Dell, A. (2006) *Methods Enzymol.* **415,** 59–86
16. Pang, P. C., Tissot, B., Drobnis, E. Z., Morris, H. R., Dell, A., and Clark, G. F. (2009) *J. Proteome Res.* **8,** 4906–4915
17. Lagrange, A. H., Botzolakis, E. J., and Macdonald, R. L. (2007) *J. Physiol.* **578,** 655–676
18. Hamill, O. P., Marty, A., Neher, E., Sakmann, B., and Sigworth, F. J. (1981) *Pflugers Arch.* **391,** 85–100
19. Lema, G. M., and Auerbach, A. (2006) *J. Physiol.* **572,** 183–200
20. Fisher, J. L., and Macdonald, R. L. (1997) *J. Physiol.* **505,** 283–297
21. Tang, X., Hernandez, C. C., and Macdonald, R. L. (2010) *J. Neurophysiol.* **103,** 1007–1019
22. Brejc, K., van Dijk, W. J., Klaassen, R. V., Schuurmans, M., van Der Oost, J., Smit, A. B., and Sixma, T. K. (2001) *Nature* **411,** 269–276
23. Guex, N., and Peitsch, M. C. (1997) *Electrophoresis* **18,** 2714–2723
24. Schwede, T., Kopp, J., Guex, N., and Peitsch, M. C. (2003) *Nucleic Acids Res.* **31,** 3381–3385
25. Case, D. A., Cheatham, T. E., III, Darden, T., Gohlke, H., Luo, R., Merz, K. M., Jr., Onufriev, A., Simmerling, C., Wang, B., and Woods, R. J. (2005) *J. Comput. Chem.* **26,** 1668–1688
26. Hornak, V., Abel, R., Okur, A., Strockbine, B., Roitberg, A., and Simmerling, C. (2006) *Proteins* **65,** 712–725
27. DeMarco, M. L., and Woods, R. J. (2008) *Glycobiology* **18,** 426–440
28. Kasturi, L., Eshleman, J. R., Wunner, W. H., and Shakin-Eshleman, S. H. (1995) *J. Biol. Chem.* **270,** 14756–14761
29. Kasturi, L., Chen, H., and Shakin-Eshleman, S. H. (1997) *Biochem. J.* **323 (Pt 2),** 415–419
30. Mellquist, J. L., Kasturi, L., Spitalnik, S. L., and Shakin-Eshleman, S. H. (1998) *Biochemistry* **37,** 6833–6837
31. Gorrie, G. H., Vallis, Y., Stephenson, A., Whitfield, J., Browning, B., Smart, T. G., and Moss, S. J. (1997) *J. Neurosci.* **17,** 6587–6596
32. Gallagher, M. J., Shen, W., Song, L., and Macdonald, R. L. (2005) *J. Biol. Chem.* **280,** 37995–38004
33. Gallagher, M. J., Ding, L., Maheshwari, A., and Macdonald, R. L. (2007) *Proc. Natl. Acad. Sci. U.S.A.* **104,** 12999–13004
34. Chou, P. Y., and Fasman, G. D. (1974) *Biochemistry* **13,** 222–245
35. Misumi, Y., Misumi, Y., Miki, K., Takatsuki, A., Tamura, G., and Ikehara, Y. (1986) *J. Biol. Chem.* **261,** 11398–11403
36. Lippincott-Schwartz, J., Yuan, L. C., Bonifacino, J. S., and Klausner, R. D. (1989) *Cell* **56,** 801–813
37. Nishizaki, T. (2003) *Brain Res. Mol. Brain Res.* **114,** 172–176
38. Monk, S. A., Williams, J. M., Hope, A. G., and Barnes, N. M. (2004) *Biochem. Pharmacol.* **68,** 1787–1796
39. Ehya, N., Sarto, I., Wabnegger, L., and Sieghart, W. (2003) *J. Neurochem.* **84,** 127–135
40. Unwin, N. (2005) *J. Mol. Biol.* **346,** 967–989
41. Unwin, N., Miyazawa, A., Li, J., and Fujiyoshi, Y. (2002) *J. Mol. Biol.* **319,** 1165–1176
42. Bocquet, N., Nury, H., Baaden, M., Le Poupon, C., Changeux, J. P., Delarue, M., and Corringer, P. J. (2009) *Nature* **457,** 111–114
43. Hilf, R. J., and Dutzler, R. (2009) *Nature* **457,** 115–118
44. Kash, T. L., Jenkins, A., Kelley, J. C., Trudell, J. R., and Harrison, N. L. (2003) *Nature* **421,** 272–275
45. Kash, T. L., Dizon, M. J., Trudell, J. R., and Harrison, N. L. (2004) *J. Biol. Chem.* **279,** 4887–4893
46. Schofield, C. M., Jenkins, A., and Harrison, N. L. (2003) *J. Biol. Chem.* **278,** 34079–34083
47. Shen, X. M., Ohno, K., Tsujino, A., Brengman, J. M., Gingold, M., Sine, S. M., and Engel, A. G. (2003) *J. Clin. Invest.* **111,** 497–505
48. Tanaka, M., Olsen, R. W., Medina, M. T., Schwartz, E., Alonso, M. E., Duron, R. M., Castro-Ortega, R., Martinez-Juarez, I. E., Pascual-Castroviejo, I., Machado-Salas, J., Silva, R., Bailey, J. N., Bai, D., Ochoa, A., Jara-Prado, A., Pineda, G., Macdonald, R. L., and Delgado-Escueta, A. V. (2008) *Am. J. Hum. Genet.* **82,** 1249–1261